Soft Matter

# Fluorescent Patterning of Paper Through Laser Engraving



| | |
|---|---|
| Journal: | *Soft Matter* |
| Manuscript ID | SM-ART-05-2020-000988.R2 |
| Article Type: | Paper |
| Date Submitted by the Author: | 07-Jul-2020 |





| | |
|---|---|
| Complete List of Authors: | Clark, Kaylee; Colorado State University, Chemistry<br>Skrajewski, Lauren; Clemson University, Chemistry<br>Benavidez, Tomas; INFIQC<br>Mendes, Leticia; USP<br>Bastos, Erick; Instituto de Química-Universidade de São Paulo, Departamento de Química Fundamental<br>Dörr, Felipe; University of São Paulo, School of Pharmaceutical Science, Department of Clinical and Toxicological Analysis<br>Sachdeva, Rakesh; Clemson University, Department of Chemistry<br>Ogale, Amod; Clemson Univ,<br>Paixao, Thiago; Instituto de Química-Universidade de São Paulo, Departamento de Química Fundamental<br>Garcia, Carlos; Clemson University, Chemistry |

# Fluorescent Patterning of Paper Through Laser Engraving

Kaylee M. Clark,[1] Lauren Skrajewski,[1] Tomás E. Benavidez,[1,2] Letícia F. Mendes,[3] Erick L. Bastos,[3] Felipe A. Dörr,[4] Rakesh Sachdeva,[1] Amod A. Ogale,[5] Thiago R.L.C. Paixão,[3*] and Carlos D. Garcia[11]

[1]*Department of Chemistry, Clemson University, Clemson SC 29634, USA*

[2]*INFIQC-CONICET, Department of Physical Chemistry, School of Chemistry, National University of Córdoba, X5000HUA Córdoba, Argentina*

[3]*Institute of Chemistry, Department of Fundamental Chemistry, University of São Paulo, 05508-000, São Paulo, SP, Brazil*

[4]*Faculty of Pharmaceutical Science, Department of Clinical and Toxicological Analyses, University of São Paulo, 05508-000, São Paulo, SP, Brazil*

[5]*Chemical Engineering and Center for Advanced Engineering Fibers and Films, Clemson University, Clemson, SC 29634, USA*

[1]To whom correspondence should be addressed.

- Institute of Chemistry, Department of Fundamental Chemistry, University of São Paulo, 05508-000, São Paulo, SP, Brazil, trlcp@iq.usp.br
- 211 S. Palmetto Blvd, Clemson, SC 29634, USA. Phone: (864) 656-1356, E-mail: cdgarci@clemson.edu

**Abstract**

While thermal treatment of paper can lead to the formation of aromatic structures via hydrothermal treatment (low temperature) or pyrolysis (high temperature), neither of these approaches allow patterning the substrates. Somewhere in between these two extremes, a handful of research groups have used $CO_2$ lasers to pattern paper and induce carbonization. However, none of the previously reported papers have focused on the possibility to form fluorescent derivatives via laser-thermal engraving. Exploring this possibility, this article describes the possibility of using a $CO_2$ laser engraver to selectively treat paper, resulting in the formation of fluorescent compounds, similar to those present on the surface of carbon dots. To determine the most relevant variables controlling this process, 3MM chromatography paper was treated using a standard 30W $CO_2$ laser engraver. Under selected experimental conditions, a blue fluorescent pattern was observed when the substrate was irradiated with UV light (365 nm). The effect of various experimental conditions (engraving speed, engraving power, and number of engraving steps) were investigated to maximize the fluorescence intensity. Through a comprehensive characterization effort, it was determined that 5-(hydroxymethyl)furfural and a handful of related compounds were formed (varying in amount) under all selected experimental conditions. To illustrate the potential advantages of this strategy, that could complement those applications traditionally developed from carbon dots (sensors, currency marking, etc.), a redox-based optical sensor for sodium hypochlorite was developed.

## 1. INTRODUCTION

The synthesis of carbon-based nanomaterials, particularly carbon dots, has attracted interest in the analytical community due to their unique fluorescent properties. Initially described by Sun[1], carbon dots are strong blue emitters when exposed to UV light.[2, 3] These optical properties stem from their composition, small dimensions (<5 nm),[3-5] and their surface chemistry.[3, 6] Carbon dots can be synthesized by laser ablation of graphite,[1, 7, 8] electrochemical treatment of carbon nanotubes,[9] thermal oxidation of molecular precursors (acetic acid, citric acid, glucose, or uric acid),[4-6, 9-13] extraction from candle soot,[14] proton beam irradiation of nanodiamonds,[15] or microwave synthesis.[16] These procedures offer tremendous versatility to the experimental design applied to their fabrication. Carbon dots are also known for their low toxicity and high chemical stability.[2, 12, 17, 18] These properties make them suitable targets for the development of promising applications including bioimaging,[2, 3, 5, 19] multicolor labeling,[5, 20] drug delivery,[2] and nanosensors.[3, 20]

It has been proposed that besides their size and surface defects, the fluorescence of carbon dots can be attributed to the presence of a variety of $sp^2$-hybridized structures containing oxygen. These aromatic structures can be prepared and purified to display specific band-gaps.[5, 21] It is also known that a number of individual polycyclic aromatic hydrocarbons (anthracene, pyrene, and perylene) display similar fluorescence properties than carbon dots.[22] Regardless of their structure, one common problem affecting the use of carbon-derived fluorescent compounds is the difficulty associated with patterning substrates using them. In an attempt to solve this problem, Zhu *et al.* developed a printable carbon dot ink from hydrothermal treatment of citric acid and ethylenediamine.[20] While these strategies and other similar printing approaches[23, 24] addressed specific needs, they still require multiple synthetic/preparation steps and dispersants before the resulting material can be uniformly deposited in substrates.

Aiming to provide a more general alternative to pattern fluorescence compounds that can be applied to develop analytical applications, this manuscript describes a quick and simple method to produce fluorescent compounds directly on the paper substrate, sharing many of the advantageous properties of

carbon dots, but without the necessity of extreme synthetic conditions. To demonstrate the potential advantages towards the development of sensors, the proposed compounds were applied to the analysis of bleach, at concentrations relevant to disinfection purposes.

## 2. MATERIALS AND METHODS

**2.1 Reagents and Solutions.** All aqueous solutions were prepared using deionized water (18 MΩ·cm; NANOpure Diamond, Barnstead; Dubuque, IA) and analytical reagent grade chemicals. Whatman 3 MM Chromatography Paper (189 $g \cdot m^{-2}$) was obtained from GE Healthcare (Pittsburgh, PA). The pH of different solutions was adjusted using either 1 M NaOH or 1 M HCl and measured using a glass electrode and a digital pH meter (Orion 420A+, Thermo; Waltham, MA). Unless otherwise stated, all chemicals were purchased from Sigma-Aldrich and used without further purification.

**2.2 Instruments.** Experiments were performed using commercial $CO_2$ laser engraver (Mini 24, 30W, Epilog Laser Systems, Golden, CO, USA) with a wavelength of 10.6 μm. The laser is controlled by a software interface, which allows setting the marking path, the scanning direction, and the conditions selected for the engraving process. The instrument has two engraving modes: raster and vector. The raster mode is used for making the engravings investigated in this paper and reaches a top speed of 2200 mm $s^{-1}$. The vector mode is used to cut through substrates, specifically in this project for cutting out engraved circles to be measured by the fluorimeter and reaches a top (lateral) speed of 90 $mm.s^{-1}$. Additional control experiments were performed using a second $CO_2$ laser cutter system (Work Special Laser, 10.6 μm) featuring a pulse duration of ~14 μs. Fluorescence patterns were obtained under UV illumination (365 nm) using a hand-held lamp and a digital camera.

**2.3 Methodology.** The formation of the fluorescent aromatic compounds was induced by laser-heat treatment of paper. In order to define spots, the laser was set to “raster” mode.[25] This mode allows defining features on the substrate with up to 600 dpi resolution. It is important to mention that although the maximum resolution in the raster mode is 1200 dpi, such resolution results in significant damage to the substrate. As described elsewhere[25], the raster engraving mode allows controlling the speed (lateral

translation of the beam) and the power (% of 30W) applied on the paper surface. These two variables allow controlling the energy density delivered to the surface per unit time. In other words, the faster the speed/the lower the power, the lower the amount of energy. For the experiments described in this manuscript, an array of circles (d = 6.35 mm) was typically produced. In order to identify the compounds formed and characterize their optical/chemical response, the engraved pattern was washed with DI water. The resulting solution was analyzed by HPLC using UV-Vis, fluorescence, and mass spectrometric detectors.

**2.4 Excitation-emission matrix fluorescence spectroscopy.** Fluorescence spectra were acquired on a Varian Cary Eclipse spectrofluorometer equipped with a microplate reader. The sheet of paper was placed on the reading plate and the emission spectra were registered from 300 nm to 700 nm at a scan speed of 600 nm $min^{-1}$; excitation (EX) slit: 10 nm, emission(EM) slit: 20 nm, and photomultiplier voltage: 600 W. Experiments were carried out in 3D mode and the excitation was automatically varied from 280 nm to 480 nm in 10 nm intervals. The spectral profile of the excitation lamp was corrected automatically, but no filter was used to correct the emission scans. The Rayleigh-Tyndall scattering resulting in intense signal along the EX/EM diagonal was removed from the excitation-emission map (EEM) by using band deconvolution as implemented in the Origin (OriginLab) software.

**2.5 Chromatographic analysis.** To characterize the compounds formed during the engraving process, two sets of chromatography experiments were performed. As a first approach, the fluorescent compounds formed by laser engraving (varying the number of engravings at 20% power and 95% speed) were extracted in DI water and analyzed via HPLC with FLD detection ($\lambda_{EX}$ = 370 nm / $\lambda_{EM}$ = 450 nm). In this case, a $C_{18}$ column (150 x 3 mm, 3 µm; BDS Hypersil; Thermo Scientific) was used and the separation was performed in isocratic mode using a mixture of water-acetonitrile (95:5) at a flow rate of 1.0 $mL.min^{-1}$.

In order to further separate the compounds formed and identify the structures of the components responsible for the fluorescence, complementary HPLC-HRMS-PDA-FD data were acquired on a Shimadzu Prominence liquid chromatograph coupled to a Bruker Daltonics microTOF-QII mass

spectrometer equipped with an electrospray source and to a PDA SPD-M20A and a FD RF-10AxL ($\lambda_{EX}$ = 370 nm / $\lambda_{EM}$ = 450 nm) detectors. In this case, samples were prepared by adding 15 mL of water to 90 mg of paper and submitting the mixture to stirring using a thermomixer (30 min, 25 ºC, 600 rpm). The samples were then centrifuged (10,000 ×g, 25 ºC, 5 min), the supernatant was filtered (PTFE filter, 0.22 µm pore) and the resulting solutions were analyzed with a Luna C18(2) column (150 × 2 mm, 3 µm; Phenomenex®) at 0.25 mL $min^{-1}$ and 30 °C under isocratic 5% B for 5 min followed by a gradient from 5 to 90% B over 15 min (solvent A: water; solvent B: acetonitrile, both containing 0.1% v/v formic acid). The delay in the retention time of the MS and FL detectors was determined using caffeine as standard.

## 3. RESULTS AND DISCUSSION

**3.1 Characterization of the fluorescence response.** Irradiation of cellulose using a $CO_2$ laser results in paper engraving through controlled thermal decomposition of the biopolymer. Irradiation of the engraved paper with UVA-blue light (350 – 405 nm) allows the recognition of the pattern fabricated on paper (Figure 1a and b). A simple experiment performed as paper chromatography using aqueous methanol (50%) as eluent, revealed that the components produced upon laser irradiation are both fluorescent and polar (Figure 1c).

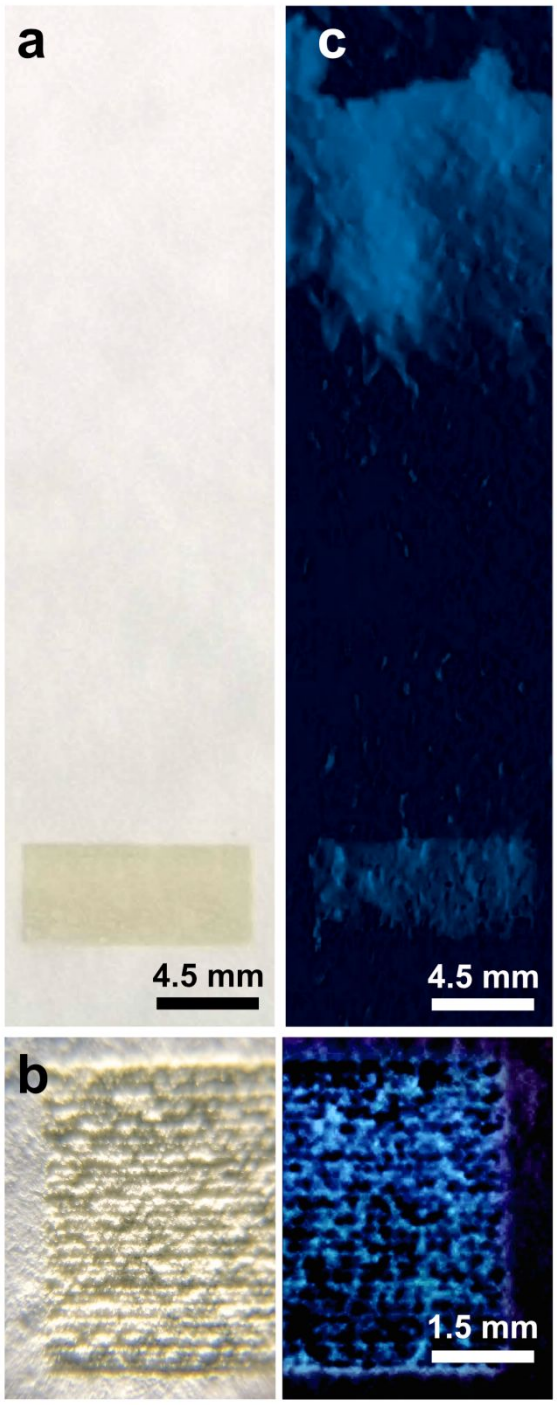


**Figure 1:** Thermal-laser engraving of cellulose. (a) Engraved cellulose under white light. (b) Image magnification (3×) and corresponding fluorescence emission ($\lambda_{EX}$ = 365 nm). (c) Fluorescence of the sample after paper chromatography (elution aqueous methanol 50%

v/v). A digital orange filter was applied to all fluorescence images to eliminate the reflected violet/blue light; the emission was pseudo-colored in blue, for clarity.

Aiming to characterize the fluorescence response, we extracted the polar fluorescent compounds from the engraved paper using aqueous methanol and registered their excitation and emission spectra in solution (Figure 2a). As it can be observed, the excitation maximum wavelength ($\lambda_{EX}$) is located at 365 nm, leading to a broad fluorescence band with maximum emission wavelength ($\lambda_{EM}$) at around 440 nm. Excitation of the engraved paper at the same wavelength leads to similar emission profile (Figure 2b). Although the emission maximum wavelength of single-type entities, e.g., molecules or single-sized carbon dots, does not depend on the excitation wavelength,[26] the emission maxima shifted towards longer wavelengths as excitation wavelength was varied from 300 nm to 480 nm. The drop in the fluorescence intensity observed, as the excitation wavelength is varied from 370 nm to 480 nm, suggests that polar species represent the main component to the emission process. Un-irradiated paper samples are virtually not fluorescent under these experimental conditions.[27]

Fluorescence excitation-emission matrix (EEM) spectroscopy shows that the maximum excitation/emission of engraved paper is located at around 350/420 nm (Figure 2c). Such diagonal dependence between the excitation and emission has been observed in carbon dots[28, 29] or biochars[30] due to the presence of multiple emissive species.[5, 6, 18, 19, 22, 31] The synchronized excitation-emission spectrum of the engraved paper was registered using a $\Delta\lambda$ of 40 nm to resolve the superimposed signals in the EEM (Figure 2d). There are multiple inflections which are better resolved in the inverse second derivative spectrum. At least four different components contribute for the fluorescence emission in the 300 to 540 nm range. Based only on these results, one could attribute the fluorescence of engraved paper to a combination of small organic molecules and emissive nanometric carbonized aggregates.[32, 33] However, the time scale and experimental conditions selected for the described engraving process is unlikely to render carbon dots.[34, 35]

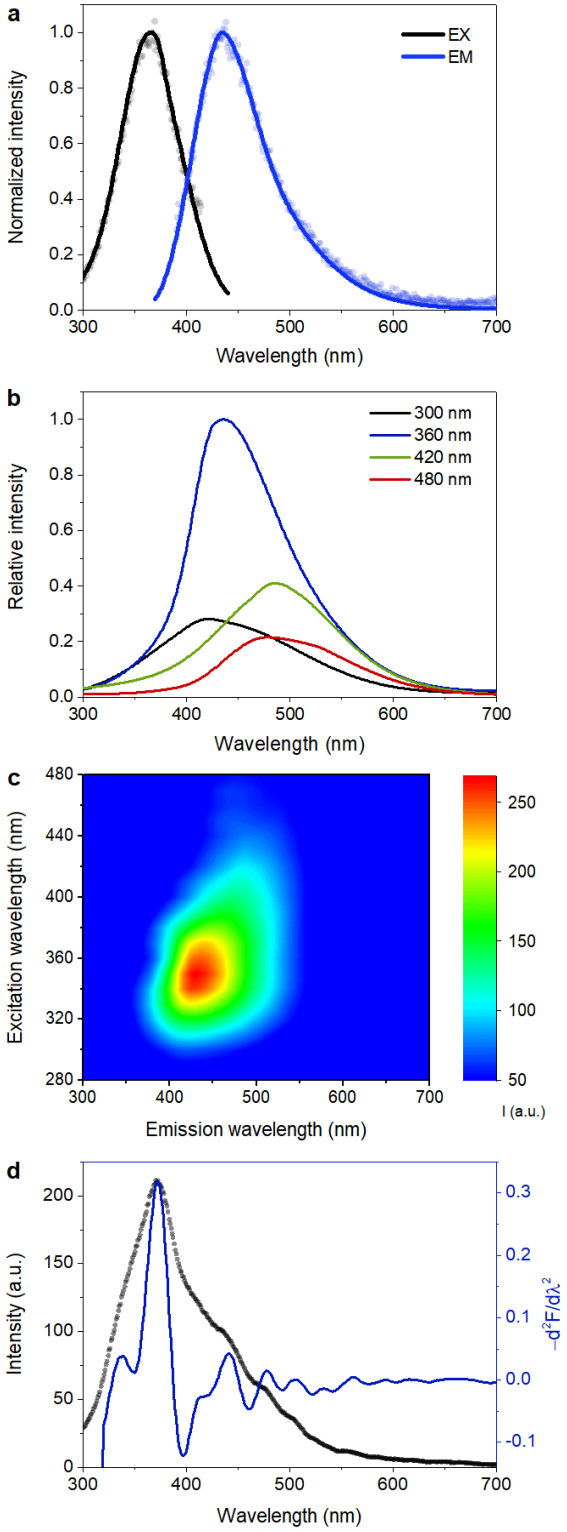


**Figure 2:** Emission properties of engraved paper. (a) Excitation (EX) and emission (EM) spectra of polar compounds extracted from thermal-laser

engraved paper. Smoothed curves (solid lines) are presented over the experimental points for clarity. $\lambda_{EX}$ = 360 nm; $\lambda_{EM}$ = 420 nm, aqueous methanol 50% v/v. (b) Fluorescence spectra of engraved paper excited at selected wavelengths. (c) Excitation-emission matrix (EEM) of the engraved paper. Non-irradiated paper (negative control) are not emissive under these experimental conditions. (d) Synchronized fluorescence spectrum of engraved paper ($\Delta\lambda$ = 40 nm) and second derivative synchronized spectrum (blue).

**3.2 Effect of engraving conditions on the fluorescence Intensity.** As the initial step to understand the formation of the fluorescent derivatives on paper, the effect of the conditions selected for the engraving process (speed, power, number of passes) were systematically investigated. The thermal degradation of the cellulose is a complex process involving multiphase reactions, various chemical pathways, the formation of unstable intermediates, and both heat and mass transfer effects.[36] Assuming that the thermal-laser degradation of cellulose shows similar behavior, it is reasonable to hypothesize that the formation of the fluorescent compounds could be controlled by adjusting the parameters of the laser engraving process. Therefore, to enhance the fluorescence of engraved paper we varied the speed and power used during the laser engraving step. The fluorescence intensity increases with the increase of the laser power (Figure 3a). These results indicate that at least a power of 4.5W (15% of 30W) is required to produce the fluorescent decomposition products and that the lateral speed (varied in the 80-95% range) only had marginal effects. The effects of both speed and power were preliminarily investigated beyond the described ranges. However, these limits were selected as a compromise between the minimum energy to produce a measurable effect (not enough heat) and the possibility to completely carbonize the paper (produced by the fast and excessive heating by the laser[37]). Based on these findings, 20% power and 95% speed were selected as the optimal parameters to maximize the formation of the fluorescent species on the paper.

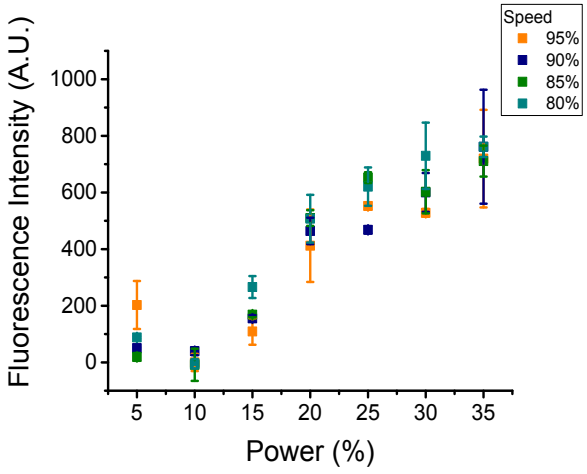


**Figure 3a:** Effect of incident power and lateral speed on the resulting fluorescence intensity. The fluorescence was found to be optimized at 20% power and 95% speed.

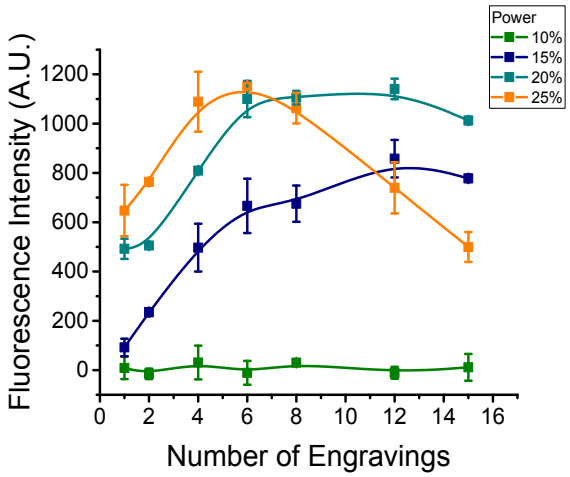


**Figure 3b**: Effect of the number of engraving steps on the fluorescence intensity. Experiments performed using 95% speed.

To increase the fluorescence with minimal cellulose carbonization, the paper was subjected to repeated engravings. This strategy allowed the paper to cool down between the engraving steps, therefore boasting the fluorescence intensity without damaging the paper (as observed at higher powers and/or lower speeds). As it can be observed in Figure 3b, the number of engravings did not yield to any improvements in fluorescence when 3W (10% of 30W) of laser power were used, suggesting that a minimum temperature was required to initiate the process. When higher laser power intensities were used (15% and 20%), a proportional increase in the intensity as a function of the number of engraving steps was observed. These results suggest that in these cases, the energy delivered to the substrate was sufficient to induce the formation of the fluorescent compounds and that (when the paper was allowed to cool down) additional engraving steps could be used without significantly damaging the paper. This effect reached a plateau after either 6 or 12 engraving steps performed at either 20% or 15% power, respectively. In comparison, when 25% power was used, a much more pronounced dependence of the fluorescence intensity with respect to the number of engravings was observed. In this case, after only 6 engraving steps, the paper began to burn, and the ablation overcomes the formation of the fluorescent compounds. Additional experiments, following the fluorescence intensity as a function of the number of engraving steps, but performed at different speeds (in the 80% - 95% range) shown the expected

increase in fluorescence as the number of engraving steps were increased (Figure SI 1a). Based on these experiments, a power of 20%, a lateral speed of 95%, and 12 engraving steps were selected as the optimum conditions to engrave the paper and maximize the formation of the fluorescence. A representative image of the paper engraved under different experimental conditions (number of engraving passes and incident power) is shown in Figure 4.

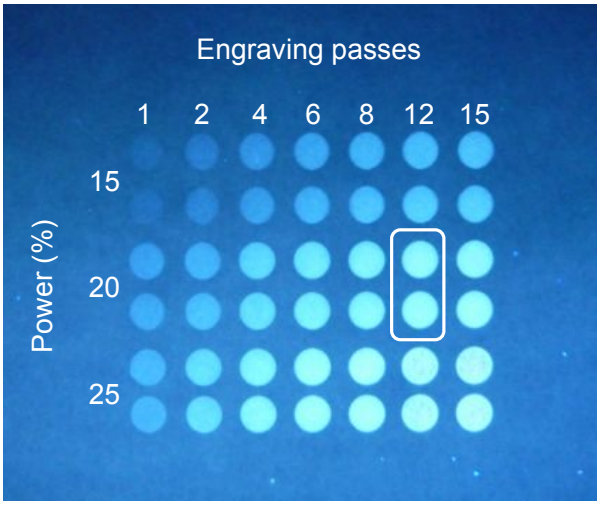


**Figure 4:** Representative image of increasing number of engravings at varying power and fixed speed of 95%. Photograph was taken under 365 nm light.

It is also important to mention that while this manuscript is focused on the chemical changes of the paper after laser engraving, tensile tests revealed a reduction in the strength of the paper as the number of passes increased. These experiments showed that at 48% of the original tenacity (3250 $N.m^{-1}$) was retained after 15 engraving passes (1546 $N.m^{-1}$, performed at 95% speed and 20% power, Figure SI 2a and 2b).

**3.3 Characterization of the compounds formed.** The laser-thermal degradation of the cellulose is known to produce a number of retro-aldol products, dehydrated species (including furfural and 5-HMF), and anhydro monosaccharides[36] which are known to show fluorescence properties. Engraving under different experimental conditions influences the fluorescence intensity, but not in the emission wavelength. This observation was also confirmed by determining the maxima for the emission spectra of

samples prepared using a power of 20%, a lateral speed of 95%, and different numbers of engraving steps (up to 30). These results (which are summarized in Figure SI 1b) supported the notion that a similar profile of compounds was formed across the experimental landscape.

To confirm this hypothesis and understand the effect of the engraving variables on the reaction pathway, paper samples engraved under different conditions, rinsed with DI water and the resulting solution was analyzed by HPLC with fluorescence detection ($\lambda_{EX}$ = 365 nm / $\lambda_{EM}$ = 440 nm). As it can be observed in Figure 5**,** increasing the number of engraving steps did not result in the formation of different species or affected their relative concentrations. In this case, and in agreement with Figure 4, it can be concluded that substrates engraved under different experimental conditions only showed differences in the fluorescence intensity but not in the compounds formed. These findings are important because by higher fluorescence intensities could allow much greater sensitivity in analytical applications.[4, 19]

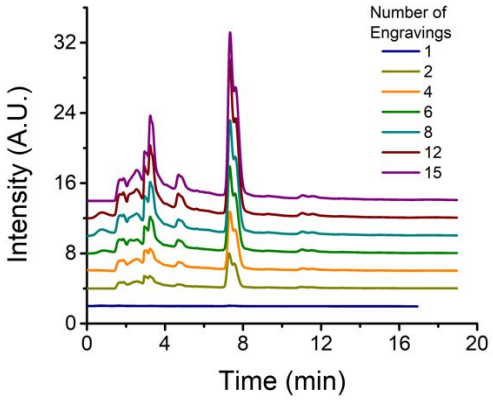


**Figure 5:** HPLC-FD analysis of the compounds formed by laser engraving (varying the number of engravings at 20% power and 95% speed) and extracted in $H_2O$.

The compounds responsible for the fluorescence were characterized by HPLC-HRMS-PDA-FD. In addition, and with the objective of highlighting the unique features of the proposed process, extracts from paper samples subjected to pyrolysis (slower process reaching higher temperatures) were also analyzed. Representative examples of the results obtained are included in Figure SI 3 (chromatograms). In this case, two large groups of compounds were identified and analyzed by HRMS. Five main components were identified in the first group of compounds (with retention times between 8.0 and 8.5 min, Figure SI

4). As shown in Figure 6, the ions with m/z 127.0393 and 145.0494 are compatible with the expected exact mass of 5-(hydroxymethyl)furfural in the protonated form and in the hydrated forms. The ions with m/z 325.1127 ($C_{12}H_{21}O_{10}$), 487.1654 ($C_{18}H_{31}O_{15}$) and 649.2188 ($C_{24}H_{41}O_{20}$), attributed to tetrahydrofuran-2-carbaldehydes, are formed by the oxidation of polymeric hexoses and are expected to be non-fluorescent due to the lack of conjugation. It is important to state that furfural (formed by two sequential dehydration steps of cellulose) was not detected in these experiments.

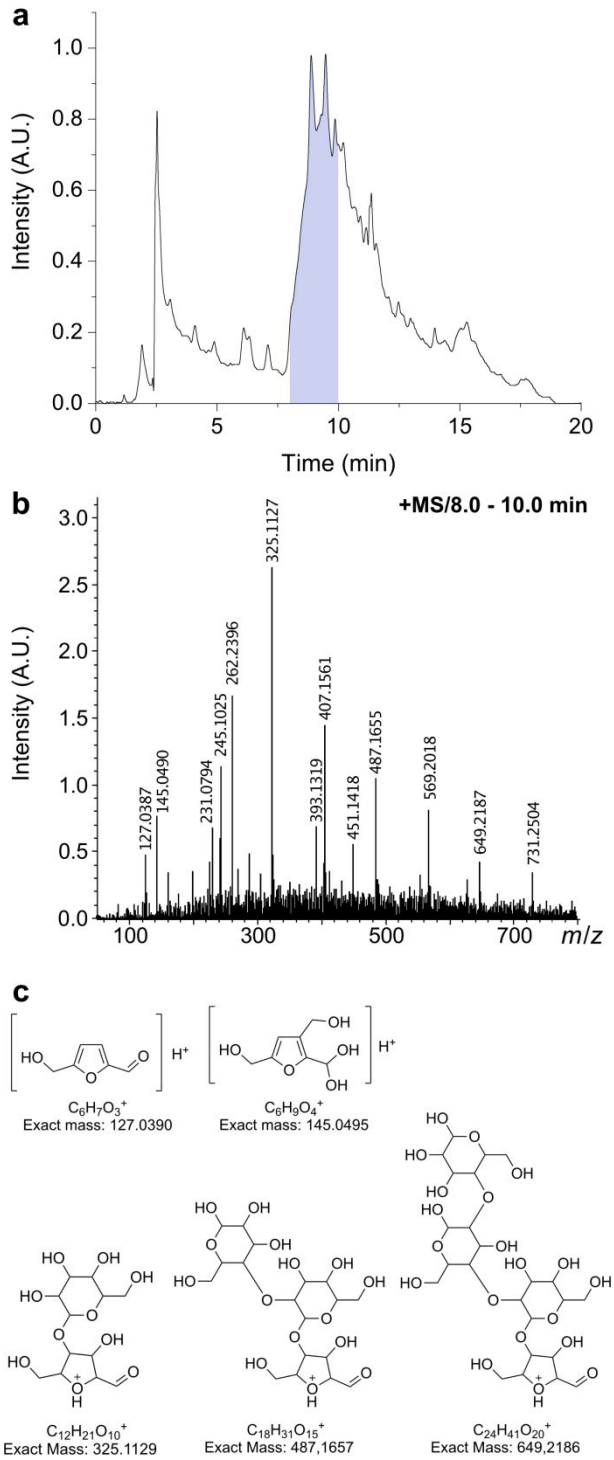


**Figure 6:** Characterization of the fluorescent species in engraved paper by HPLC-HRMS-PDA-FD. (a) Chromatogram obtained with fluorescence detection ($\lambda_{EX}$ = 370 nm / $\lambda_{EM}$ = 450 nm). The blue filling indicates the region of higher fluorescence intensity. (b) Mass spectra of the species with retention time ranging from 8 to 10 min. (c) Chemical structures of species with exact mass compatible with the experimental *m*/*z*.

The formation of these compounds is also in line with previous reports describing that heating filter papers above 160 $^{o}$C allowed the formation of a multitude of new chromophores.[38, 39] It is also important to state that although determining the fluorescence mechanism in such complex system would require a number of additional studies,[40] our results suggest that fluorescence in our samples can be attributed to conventional radiative excited state deactivation from the formed furfural derivatives. These structures display a signal that is different from the orange-red luminescence from dots formed by aggregates of furfural derivatives (10 min synthesis).[41]

**3.4 Response of the compounds formed.** In order to illustrate the potential of the approach towards the development of an application, the dependence of the fluorescence intensity with respect to the pH was first investigated. In this case, a 0.1M $Na_3PO_4$ solution was titrated with HCl to prepare solutions of various pH values ranging from 1-13. These solutions were then placed on the engraved areas of paper (fabricated using 20% power, 95% speed, 15 times), allowed to dry at room temperature, and finally measured using the previously described approach. As it can be observed in **Figure SI 5**, the fluorescence emission (intensity and $\lambda_{MAX}$) of the engraved areas remained largely unchanged under these conditions.

On the contrary, it was observed that solutions containing sodium hypochlorite were able to cause significant decreases in the fluorescence of the laser-engraved papers (Figure SI 6). As shown in Figure 7a, the fluorescence quenching of the engraved paper was found to be dependent of the hypochlorite concentrations in the range between 0 – 0.1 mM. Beyond that concentration, the fluorescence was totally quenched. The sensitivity and limit of detection ($3\sigma$/sensitivity) of the method, estimated from the Stern-Volmer plot (Figure 7a), was 0.0149 $\mu M^{-1}$ ($R^2$= 0.989) and 7.7 $\mu$M, respectively. Although the proposed strategy covers a narrower range of concentrations than other commercial fluorometric assays (0.002 – 100 mM),[42] the simplicity and low-cost of the proposed procedure makes this approach particularly attractive towards sensing. It is worth emphasizing that our samples did not require any purification process before the reaction with hypochlorite[39] and allows patterning paper via direct writing.

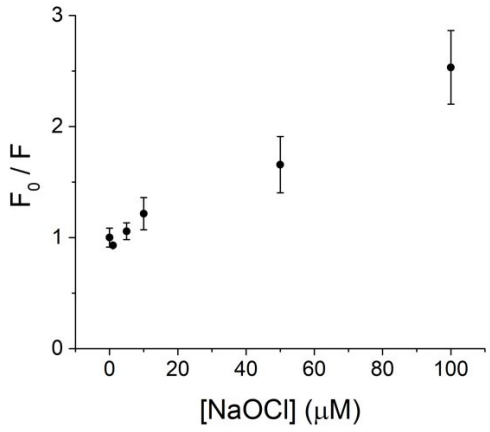


**Figure 7a:** Dependence of the fluorescence quenching with respect to the concentration of sodium hypochlorite. Paper was treated with 20% power, 95% speed for 15 engravings. 4 µL of hypochlorite solutions were added to the rastered spots of paper. Fluorimeter Excitation: 365 nm, Emission: 440 nm (n=4)

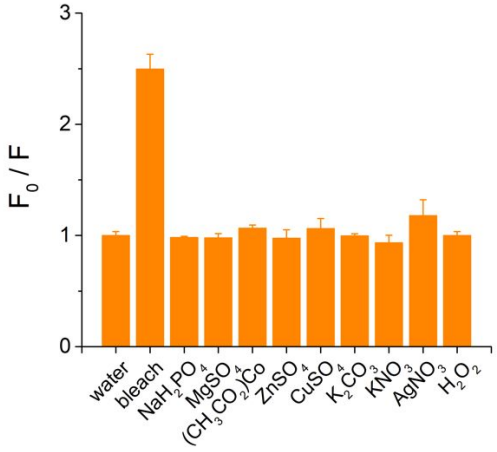


**Figure 7b**: Effect of common interferents at a concentration of 10 mM (n=3) on the fluorescence quenching of laser-engraved paper samples.

It was also observed that other compounds, including $H_2O_2$, which are known to affect the signal of some carbon dots via quenching did not affect the fluorescence of the engraved paper (Figure 7b). These results are in agreement with previous reports[43] that have attributed this behavior to the oxidation of -OH groups of the fluorescent molecules.

Based on the importance of hypochlorite in medical hygiene but also considering its toxicological and environmental effects, many fluorescent probes[44, 45] have been studied for its detection and/or quantification. In this context, the procedure here described represents a quantitative, simple and fast alternative to these applications. It is also important to note that this application was selected only to demonstrate the applicability of the approach and not to develop a sensor to compete with the analytical performance of other approaches. Since the novel human coronavirus SARS-CoV-2 (COVID-19) has spread around the world, household disinfectants such as bleach have been in high demand because of their effective inactivation of the COVID-19 virus from contaminated surfaces where the virus can remain viable for days. To prevent sustained transmission, the World Health Organization (WHO) has

recommended the use of 13 – 67 mM sodium hypochlorite solutions[46] for cleaning and disinfecting surfaces. Our devices could be conveniently used to identify (after the corresponding dilution) hypochlorite solutions that are suitable for disinfection or used as fluorescent stickers to be sprayed as controls over surfaces to be disinfected. Therefore, the present article introduces a fast and simple procedure for quality control of these solutions and procedures.

## 4. CONCLUSIONS

The experiments described in this paper demonstrated that a soft thermal treatment of 3MM chromatography paper using a standard $CO_2$ laser produces a series of low MW fluorescent compounds. In line with the kinetics of the reactions involved,[47] this fast and low-temperature process is unlikely to allow the *in-situ* formation of carbon dots, which have not been found in the structures produced. The blue fluorescence, shared by many carbon-based nanomaterials, has a maximum excitation wavelength of 365 nm and emission wavelength of 440 nm. Although our results suggest that similar compounds are formed throughout the experimental landscape investigated, the amount formed could be altered and optimized by changing parameters such as the engraving speed, the incident power of the laser, and number of engraving steps applied. The latter is a critical parameter because it allows sequentially increasing the concentration of the furfural derivatives, without ablating the surface of the paper.[37, 48] Unlike previous synthesis methods applied to the formation of carbon dots and other carbon-based fluorescent materials, our method is fast, simple, and allows patterning structures onto the paper that can be even observed with the naked eye (with the aid of UV light, of course). The formed structures can be used for the detection of sodium hypochlorite with a selectivity and sensitivity that is comparable to other carbon-based probes.

## 5. Acknowledgements

Financial support for this project has been provided in part by Clemson University, the National Science Foundation – Office of International Science and Engineering (Award #1458177) and the Brazilian

agencies FAPESP (Grant Numbers: 2018/16250-0 and 2018/08782-1), CAPES, CNPq (grant numbers: 305605/2017-8) and INCTBio (573672/2008-3).

Authors have declared no conflict of interests.

**6. References**

1. Y.-P. Sun, B. Zhou, Y. Lin, W. Wang, K. S. Fernando, P. Pathak, M. J. Meziani, B. A. Harruff, X. Wang and H. Wang, J. Am. Chem. Soc., 2006, **128**, 7756-7757.
2. S. Zhu, S. Tang, J. Zhang and B. Yang, Chem. Comm., 2012, **48**, 4527-4539.
3. J. C. E. da Silva and H. M. Gonçalves, TrAC, Trends Anal. Chem., 2011, **30**, 1327-1336.
4. H. Li, X. He, Z. Kang, H. Huang, Y. Liu, J. Liu, S. Lian, C. H. A. Tsang, X. Yang and S. T. Lee, Angew. Chem., Int. Ed., 2010, **122**, 4532-4536.
5. Y. Fang, S. Guo, D. Li, C. Zhu, W. Ren, S. Dong and E. Wang, ACS Nano, 2011, **6**, 400-409.
6. A. B. Bourlinos, A. Stassinopoulos, D. Anglos, R. Zboril, M. Karakassides and E. P. Giannelis, Small, 2008, **4**, 455-458.
7. S.-L. Hu, K.-Y. Niu, J. Sun, J. Yang, N.-Q. Zhao and X.-W. Du, J. Mater. Chem., 2009, **19**, 484-488.
8. S. Hu, J. Sun, X. Du, F. Tian and L. Jiang, Diamond Relat. Mater., 2008, **17**, 142-146.
9. J. Zhou, C. Booker, R. Li, X. Zhou, T.-K. Sham, X. Sun and Z. Ding, J. Am. Chem. Soc., 2007, **129**, 744-745.
10. R. Liu, D. Wu, S. Liu, K. Koynov, W. Knoll and Q. Li, Angew. Chem., Int. Ed., 2009, **121**, 4668-4671.
11. A. B. Bourlinos, A. Stassinopoulos, D. Anglos, R. Zboril, V. Georgakilas and E. P. Giannelis, Chem. Mater., 2008, **20**, 4539-4541.
12. Q.-L. Zhao, Z.-L. Zhang, B.-H. Huang, J. Peng, M. Zhang and D.-W. Pang, Chem. Comm., 2008, 5116-5118.

13. G. M. Durán, T. E. Benavidez, A. M. Contento, A. Ríos and C. D. García, J. Pharm. Anal., 2017, **7**, 324-331.

14. H. Liu, T. Ye and C. Mao, Angew. Chem., Int. Ed., 2007, **46**, 6473-6475.

15. S.-J. Yu, M.-W. Kang, H.-C. Chang, K.-M. Chen and Y.-C. Yu, J. Am. Chem. Soc., 2005, **127**, 17604-17605.

16. H. Zhu, X. Wang, Y. Li, Z. Wang, F. Yang and X. Yang, Chem. Comm., 2009, 5118-5120.

17. S. N. Baker and G. A. Baker, Angew. Chem., Int. Ed., 2010, **49**, 6726-6744.

18. L. Shi, J. H. Yang, H. B. Zeng, Y. M. Chen, S. C. Yang, C. Wu, H. Zeng, O. Yoshihito and Q. Zhang, Nanoscale, 2016, **8**, 14374-14378.

19. B. Kong, A. Zhu, C. Ding, X. Zhao, B. Li and Y. Tian, Adv. Mater., 2012, **24**, 5844-5848.

20. S. Zhu, Q. Meng, L. Wang, J. Zhang, Y. Song, H. Jin, K. Zhang, H. Sun, H. Wang and B. Yang, Angew. Chem., Int. Ed., 2013, **52**, 3953-3957.

21. R. Ye, Z. Peng, A. Metzger, J. Lin, J. A. Mann, K. Huang, C. Xiang, X. Fan, E. L. Samuel and L. B. Alemany, ACS Appl. Mater. Interfaces, 2015, **7**, 7041-7048.

22. M. Fu, F. Ehrat, Y. Wang, K. Z. Milowska, C. Reckmeier, A. L. Rogach, J. K. Stolarczyk, A. S. Urban and J. Feldmann, Nano Lett., 2015, **15**, 6030-6035.

23. P. Li, L. Huang, Y. Lin, L. Shen, Q. Chen and W. Shi, Nanotechnol., 2014, **25**, 055603.

24. J. Wang, C. F. Wang and S. Chen, Angew. Chem., Int. Ed., 2012, **124**, 9431-9435.

25. E. F. M. Gabriel, W. K. T. Coltro and C. D. Garcia, Electrophoresis, 2014, **35**, 2325-2332.

26. H. Wang, C. Sun, X. Chen, Y. Zhang, V. L. Colvin, Q. Rice, J. Seo, S. Feng, S. Wang and W. W. Yu, Nanoscale, 2017, **9**, 1909-1915.

27. K. H. Malinowska, T. Rind, T. Verdorfer, H. E. Gaub and M. A. Nash, Anal. Chem., 2015, **87**, 7133-7140.

28. L. Pan, S. Sun, A. Zhang, K. Jiang, L. Zhang, C. Dong, Q. Huang, A. Wu and H. Lin, Adv. Mater., 2015, **27**, 7782-7787.

29. X. Guo, Y. Zhu, L. Zhou, L. Zhang, Y. You, H. Zhang and J. Hao, RSC Adv., 2018, **8**, 38091-38099.

30. C. Yang, Y. Liu, X. Sun, S. Miao, Y. Guo and T. Li, Bioresour. Technol., 2019, **287**, 121471.

31. M. Ammam, B. Keita, L. Nadjo, I.-M. Mbomekalle and J. Fransaer, J. Electroanal. Chem., 2010, **645**, 65-73.
32. C.-R. Wang, Y.-Y. Gong, W.-Z. Yuan and Y.-M. Zhang, Chin. Chem. Lett., 2016, **27**, 1184-1192.
33. W. Zhang Yuan and Y. Zhang, J. Polym. Sci., Part A: Polym. Chem., 2017, **55**, 560-574.
34. M. L. Liu, B. B. Chen, C. M. Li and C. Z. Huang, Green Chem., 2019, **21**, 449-471.
35. N. Papaioannou, M.-M. Titirici and A. Sapelkin, ACS Omega, 2019, **4**, 21658-21665.
36. Y.-C. Lin, J. Cho, G. A. Tompsett, P. R. Westmoreland and G. W. Huber, J. Phys. Chem. C, 2009, **113**, 20097-20107.
37. W. R. de Araujo, C. M. Frasson, W. A. Ameku, J. R. Silva, L. Angnes and T. R. Paixão, Angew. Chem., Int. Ed., 2017, **129**, 15309-15313.
38. A. Emsley and G. Stevens, Cellulose, 1994, **1**, 26-56.
39. H. Tylli, I. Forsskåhl and C. Olkkonen, Cellulose, 2000, **7**, 133-146.
40. C. Xia, S. Zhu, T. Feng, M. Yang and B. Yang, Adv. Sci., 2019, **6**, 1901316.
41. V. Gude, A. Das, T. Chatterjee and P. K. Mandal, Phys. Chem. Chem. Phys., 2016, **18**, 28274-28280.
42. Abcam, Hypochlorite Assay Kit (Fluorometric) (ab219930).
43. B. Yin, J. Deng, X. Peng, Q. Long, J. Zhao, Q. Lu, Q. Chen, H. Li, H. Tang and Y. Zhang, Analyst, 2013, **138**, 6551-6557.
44. X. Chen, X. Wang, S. Wang, W. Shi, K. Wang and H. Ma, Chem. Eur. J., 2008, **14**, 4719-4724.
45. M.-Y. Li, K. Li, Y.-H. Liu, H. Zhang, K.-K. Yu, X. Liu and X.-Q. Yu, Anal. Chem., 2020, **92**, 3262-3269.
46. World Health Organization, Operational considerations for COVID-19 management in the accommodation sector: interim guidance, 31 March 2020.
47. Y. Liu, H. Huang, W. Cao, B. Mao, Y. Liu and Z. Kang, Mater. Chem. Front., 2020.
48. M. Reynolds, L. M. Duarte, W. K. Coltro, M. F. Silva, F. J. Gomez and C. D. Garcia, Microchem. J., 2020, 105067.

**Graphical Abstract**